Anbar Journal of Engineering Science (AJES) **Vol. 17 , No. 1 (2026) , pp. 14 ~ 24**
P-ISSN: 1997-9428; E-ISSN: 2706-7440 DOI: http://doi.org/10.37649/AJES-25-031

University of Anbar

Anbar Journal of Engineering Science

journal homepage: https://ajes.uoanbar.edu.iq/

Numerical Characterization of Corrugated Tube Optimum Hydrothermal Performance with Sinusoidal Wall Heat Flux

Zina M. Saleh[a] , Saad M. Jalil[b]

[a,b]*Mechanical Engineering Department, Engineering College, University of Anbar, Ramadi, Anbar, Iraq*
Email: zen23e2003@uoanbar.edu.iq ; ORCID: https://orcid.org/0009-0001-8269-3917
Email: saad.jalil@uoanbar.edu.iq ; ORCID: https://orcid.org/0000-0001-9784-4661

PAPER INFO

Paper history
Received: 08/11/2025
Revised: 12/01/2026
Accepted: 15/03/2026

Keywords:
Wavy tubes
Sinusoidal
Transient Heat flux
Parametric Study
Numerical Simulation

ABSTRACT

A computational hydrothermal analysis is conducted in order to investigate the influence of a time-varying sinusoidal wall heat flux on both thermal and hydrodynamic performance in a sinusoidally wavy tube for constant flow. Whereas most of the earlier works considered only steady thermal boundary conditions, a temporally varying sinusoidal heat flux is considered here to interact with the wavy tube geometry. First, a reference case of a smooth tube is analysed for Re between 100 and 15 000. Then, wavy tubes, with different geometrical parameters - wave height 0.1D, 0.2D, and 0.4D; wavelength 2D, 4D, and 6D; and tube length 10D, 20D, and 40D - are analysed. It means the optimal thermal performance, and its Nusselt number could enhance about 106.4% compared with the smooth tube for a wavy tube wavelength, wave height, and length corresponding to 2D, 0.4D, and 20D, respectively. This optimum configuration is then exposed to a time-varying sinusoidal heat flux of various frequencies and amplitudes. The results indicate that the time-averaged Nusselt number is marginally influenced by the frequency and amplitude of the imposed heat flux, suggesting the thermal response will be dominated by the mean heat flux rather than its instantaneous changes. These results show that oscillatory wall heating does not affect the overall thermal performance of wavy tubes within the tested parameter ranges.

1. Introduction

In thermal engineering applications, such as electronic cooling, energy recovery systems, and heat exchangers, improving heat transfer in compact systems is a crucial goal. The use of wavy (corrugated) tubes, which introduce surface periodicity to enhance flow mixing and disrupt the boundary layer, is one efficient way to improve thermal performance without significantly increasing system size or pumping power. In many applications, such geometry is superior to a standard smooth tube and can significantly enhance convective heat transfer. Several studies have focused on the potential for enhancement of the thermal performance of heat exchangers by using corrugated or wavy surfaces. These geometries-often sinusoidal curves-promote secondary flows and flow separation, which greatly increase mixing and, hence, heat transfer. Ramgadia and Saha[1] conducted a quantitative investigation of fully developed flow and heat transport in a wavy channel using a finite volume method. From the results, it can be observed that

* Corresponding author: Saad M. Jalil : Saad.jalil@uoanbar.edu.iq ; 009647800842666

the critical Reynolds number for flow unsteadiness decreases with an increase in Hmin/Hmax. Model M2 (Hmin/Hmax = 0.2) corresponds to the highest (Nu = 9.572) and (PEC = 1.765). The configurations that produce PEC values greater than unity offer promising design alternatives and reflect a net thermal-hydraulic benefit. The difference in results among the situations also shows the role of geometry when optimizing performance. Higher waviness not only improves heat transfer but also increases the friction factor, f = 7.633 for Hmin/Hmax = 0.1. This work identifies the optimum shapes for maximum enhancement in thermal performance and confirms that unsteady flow leads to significant heat transfer enhancement.Bai et al.[2] used large eddy simulations (LES) at Re = 3.0×10^3 and Pr = 0.7 to study the near wake flow and forced convection heat transfer around a sinusoidal wavy cylinder. The wavy cylinder significantly alters the wake flow, affecting Reynolds stresses and heat flux distributions, according to the results. Recirculation bubble dynamics and coherent spanwise vortices are intimately related to heat transfer performance. Reduced fluid forces (drag and lift fluctuations) and lower heat transfer efficiency (~11% less than the smooth cylinder) are two characteristics of the wavy cylinders with λ = 1.89 and 6.06. The results indicate the optimal balance between enhancing heat transfer and improving aerodynamic performance in engineering applications.

Wen et al.[3] investigated flow and heat transfer of supercritical CO_2 mixtures in a sinusoidal wavy channel of a printed circuit heat exchanger using CFD and machine learning models. Local Nusselt numbers peaked near 120 due to acceleration and changes in thermal properties around the pseudo-critical point. Ahmadpour and Abadi[4] conducted a detailed numerical analysis on gas-liquid multiphase flows in vertical sinusoidal wavy channels under both adiabatic (air-water) and condensing (R134a) conditions. Results showed up to a 40% increase in heat transfer coefficient over straight channels. However, the pressure drop increased significantly up to six times at higher mass fluxes.

Zhang et al.[5] Conducted a numerical investigation of water-based Al_2O_3 nanofluids (0-4% volume) flowing through a wavy-walled tube heat exchanger. Simulations covered wave amplitudes ranging from 0 to 2 mm and Reynolds numbers between 250 and 1000. Results indicated a 64% enhancement in convective heat transfer at a 4% concentration compared to the base fluid in a straight tube. Heat transfer was further enhanced by increasing the Reynolds number and the wave amplitude, though there was a 45% increase in pressure drop at the highest condition encountered. Al-Obaid[6] carried out a numerical investigation into heat transfer and flow performance of 3D corrugated pipes. Three models with different pitch-to-diameter ratios (P/D = 1.5, 2.0, and 2.5) were analysed for Reynolds numbers ranging from 5,000 to 25,000 within a regime of steady turbulent flow. The results show that the corrugated configuration promotes mixing and disrupts boundary layers by inducing complex secondary flows. When compared to smooth pipes, the Nusselt number rose by as much as 80%, and the friction factor increased accordingly. Zhang et al.[7] numerically analysed heat transfer and flow behaviour in wavy-walled tubes subjected to combined axial pulsation and radial vibration. The study demonstrated that this dual-mode excitation enhances turbulence and vortex formation, thereby significantly improving heat transfer. With Reynolds numbers from 100 to 500 and pulsation amplitudes between 0.2 and 1.0m, the heat transfer enhancement reached up to 36.2% over pulsation alone, and the performance evaluation criterion reached 1.26. Corcoles et al. [8] investigated heat transfer in a double-pipe heat exchanger with inner corrugated tubes of three pitch lengths and a fixed corrugation depth, both numerically and experimentally. According to the results, corrugated tubes significantly improve heat transfer. When compared to smooth tubes, the friction factor can increase by up to 36%, and the Nusselt number can increase by up to 47%.

Al-Obaidi and Alhamid[9] numerically examined turbulent Al_2O_3–water nanofluid flow in a 3D sinusoidal-wavy channel at Reynolds numbers ranging from 5,000 to 20,000 and volume concentrations of 1–3%. Results showed that both nanoparticle addition and wavy geometry enhanced heat transfer, with the average Nusselt number increasing by up to 29.8% and the thermal performance factor (TPF) reaching 1.23. The friction factor increases, which reflects a trade-off between heat transfer enhancement and pressure loss.Yoon et al.[10] investigated laminar forced convection around wavy elliptic cylinders with aspect ratios ranging from 0.5 to 2.0 and waviness amplitudes of up to 0.2. Waviness was found to enhance heat transfer by promoting vortex shedding and mixing. Mehta and Pati[11] numerically studied laminar forced convection in a

2D wavy channel, analysing thermo-hydraulic and entropy generation characteristics. Results showed that thermal effects mainly drove entropy generation, and the average Nusselt number increased with both Re and Pr. At low Re, the enhancement ratio and performance factor varied non-monotonically with Pr, but became monotonic at higher Re. Maximum heat transfer enhancement (ΔNu%) reached 429% with a pressure ratio (PR) of up to 34 times. Optimal performance occurred at high Re and Pr with short wavelengths and larger amplitudes. G. Russ and H. Beer [12] studied fully developed flow and heat transfer in a sinusoidal wavy pipe with periodically converging-diverging cross-section over a total length of 11 wavelengths. The study focuses on convective transport enhancement for a range of Reynolds numbers from laminar to turbulent flow. It uses low-Reynolds-number (LRN) k-ε turbulence models to investigate the impact of periodic surface shapes on turbulent heat and mass transfer. The findings showed that Nusselt and Sherwood numbers are strongly influenced by vortex interactions, flow separation, and turbulence structures, with maxima near reattachment points. Convective transport is improved with increasing wave amplitude (λ) and reducing wavelength (γh), but the pressure drop is increased, as established in the study. The Nusselt number exhibits local maxima in near reattachment points for laminar flow (Re = 300), but overall heat transfer remains close to that for a straight pipe. Turbulence and flow induced by shear substantially increase the Nusselt number for transitional and turbulent flows (Re = 2000–8000), with fully developed turbulent flow resulting in an improvement in heat transfer of 1.5–2 times compared to a straight pipe.

Sun and Zeng [13]used the same constraints on mass flow rate, pumping power, and pressure drop in their study, which included an experimental and numerical investigation of heat transfer in turbulent flow for three types of corrugated tubes compared to plain tubes. Under uniform heat-flux boundary conditions, the study uses air as the working fluid and considers a Reynolds number range of 4000-100,000. The results show that corrugated tubes can enhance the mean Nusselt number up to 50%. Greater heat transfer results from the combined effects of higher velocity and a temperature gradient, leading to more than a 50% enhancement in the convective contribution and decreasing the synergy angles by approximately 1-2°. Economically, the use of corrugated tubes in ground-source heat pump systems could reduce the cost index from \$0.1 to \$0.08/kJ, indicating high cost and energy savings. Based on the findings, corrugated tubes have tremendous potential for efficient thermal system design.

On the other hand, most existing numerical and experimental studies have assumed steady-state or constant heat flux boundary conditions. However, in many real-world systems, such as solar thermal collectors, internal combustion engines, and pulsating heat pipes, the thermal load is inherently unsteady and often fluctuates over time. Modelling heat flux as a time-dependent function, such as a sinusoidal wave, can better reflect realistic thermal operating conditions. Generally, very few studies have investigated the effect of time-varying (oscillating) heat flux on thermal and hydrodynamic performance. However, some researchers have addressed related topics, for example, Ahmed and Trouve[14] numerically examined the unsteady thermal response of biomass fuel particles subjected to oscillatory radiative and convective heat fluxes. Using oscillation frequencies of 0.1 and 1 Hz, they analysed charring and non-charring particles with initial half-thicknesses of 1- and 10-mm. Radiative heating showed a quasi-linear behaviour, with minimal effects on burnout and ignition times (<±4%). In contrast, convective heating with in-phase oscillations resulted in nonlinear effects, including a 70% reduction in burnout time, increased surface temperature, and enhanced mass loss. Khaled[15] analytically investigated heat conduction and entropy transfer in a semi-infinite medium and a finite wall under combined periodic heat flux and convective boundary conditions. Exact solutions for steady and oscillatory temperature components were derived. Results showed that increasing the Biot number, or decreasing the heat transfer and thermal oscillation parameters, significantly reduced temperature fluctuations.

The objective of the current study is to conduct a numerical investigation into thermal and hydrodynamic performance of a sinusoidally wavy tube subjected to a time-varying sinusoidal wall heat flux. The novelty in this work is the application of a temporally varying thermal boundary condition on the wavy tube geometry, extending previous studies that were, for the most part, conducted under either steady or constant heat flux assumptions. The influences of heat flux amplitude and frequency on heat transfer characteristics are scrutinized in detail. Such a study will involve a baseline comparison with a straight tube, followed by parametric variations in tube geometry, specifically length, wavelength, and wave height, and finally the optimized configuration under dynamic thermal loading. The findings offer new insights into designing efficient heat exchangers that operate under unsteady conditions.

2. Computational model and governing equations

In this study, the thermal and hydrodynamic behaviour of steady flow inside a wavy tube subjected to a time-varying wall heat flux, as shown in **Figure 1**, is investigated using the finite volume method. The geometry of the tube is described by a sinusoidal function in the axial direction, and the geometric dimensions are calculated from the dimensionless parameters as shown in Table 1 related to the tube diameter (D=19mm)

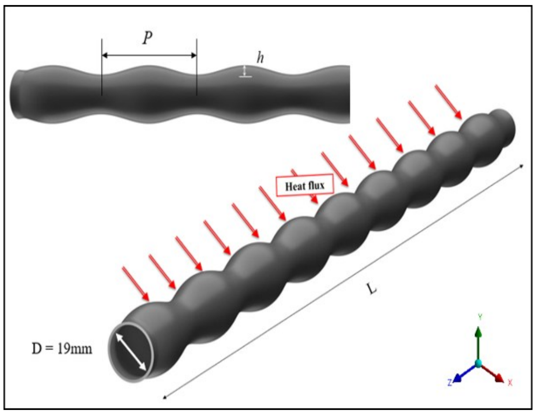

Figure 1. Geometry of sinusoidal wavy tube

Table 1. Studied tubes dimensions

Parameter	Scale	Values (mm)
Tube length (L)	$L = \begin{bmatrix}10\\20\\40\end{bmatrix} D$	190 380 760
Wavelength (P)	$P = \begin{bmatrix}2\\4\\6\end{bmatrix} D$	38 76 114
Wave Amp. (h)	$h = \begin{bmatrix}0.1\\0.2\\0.4\end{bmatrix} D$	0.475 0.95 1.9

$$y = R + \left(h * sin(2\pi) * \left(\frac{z}{P}\right)\right) \tag{1}$$

Three different wavelengths are used to assess the influence of geometric periodicity on heat transfer. For validation and comparison, a straight, smooth tube with a length of 1000 mm for the developing section and 200mm for the test section was used and also simulated. The flow is assumed to be incompressible, laminar and turbulent, steady, and Newtonian. For Reynolds numbers varying between 5000 and 15,000, the SST-kω turbulence model was used because of its capability in simulating near-wall effects and flow separation in an internal, complex geometry problem. The governing equations are the steady-state Navier–Stokes equations for momentum and the transient energy equation, and given as follows[16]:

- Continuity Equation:

$$\frac{\partial \rho}{\partial t} + \nabla \cdot (\rho u) = 0 \tag{2}$$

- Momentum equation:

$$\frac{\partial (\rho u)}{\partial t} + \nabla \cdot (\rho uu) = -\nabla p + \nabla \cdot \tau + \rho g \tag{3}$$

- Energy Equation:

$$\frac{\partial (\rho H)}{\partial t} + \nabla \cdot (\rho uH) = \nabla \cdot (k \nabla T) \tag{4}$$

Where τ is the stress tensor and ρg is the gravitational force, with the body and the total enthalpy ignored.

Since the thermal boundary condition is time-dependent, the fluid enters the domain with a fully developed velocity and temperature profiles, which are extracted from a separate simulation of a straight developing section. The simulation is transient to capture the time-dependent thermal response of the system. A second-order implicit scheme is employed for time advancement, and second-order spatial discretisation schemes are applied to the convective and diffusive terms. Pressure-velocity coupling is handled using the SIMPLE algorithm.

At the inlet, velocity and temperature profiles were extracted from the developing section and imposed as fixed inlet boundary conditions for the test section. The outlet is modelled using a zero-gauge pressure boundary condition, allowing the flow to exit the domain naturally without reflection. All tube walls are subjected to no-slip boundary conditions, and a time-dependent sinusoidal heat flux is imposed on the outer surface to simulate unsteady thermal loading. Table 2 presents the properties of the materials used.

Table 2. The properties of materials

Materials	Cp (J/kg. K)	ρ (kg/m^3)	μ (kg/m.s)	K (W/m. K)
Water	4176	995	0.000769	0.62
Copper	385	8960	-	401

2.1. Mesh Independent Test

The numerical study in this work was performed using the commercial computational fluid dynamics (CFD) software ANSYS Fluent. The 3D geometry for all cases was generated using ANSYS Design Modeler, where domains were discretised using ANSYS meshing. The computational domain is meshed using a structured mesh with refinement

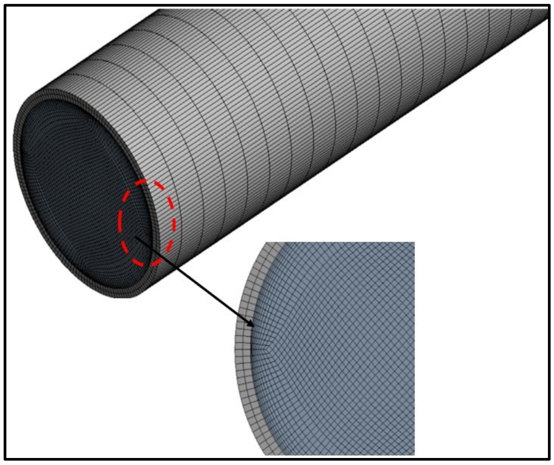

Figure2. 3D Model Mesh

near the wall regions to accurately resolve thermal gradients, as shown in Figure 2. To ensure mesh-independent results in the developing section, which its length was 1000mm, a grid independence test was conducted using seven progressively refined meshes, ranging from approximately 56520 to over 4350720 elements.

All simulations were performed at a Reynolds number of 15,000 under identical physical and boundary conditions. Following the grid independence analysis performed in the developing section, a similar study was conducted for the test section, which had a length of 200 mm, to verify the mesh sensitivity of the thermal predictions using an identical inlet velocity and temperature profiles. Based on these findings, Mesh 5 with approximately 1192320 elements was selected for all subsequent transient simulations in the test section because the mesh balances the desirable numerical accuracy with the acceptable computational cost.

Key parameters like the average Nusselt number and friction factor have been monitored for mesh convergence. From the information available in Table 3 and Figure 3, it can be seen that the Nusselt number varied noticeably among the course meshes but stabilized for Mesh 5 and finer meshes. Between Mesh 6 and Mesh 7, the variation in

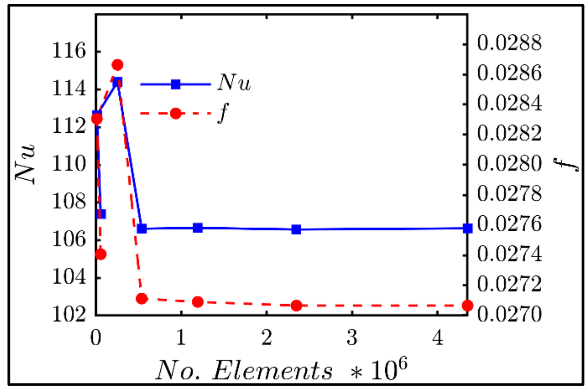

Figure 3. Grid Independent Test for Smooth Tube

Nusselt number was 0.057% and the corresponding variation in friction factor was below 3.7%. Such a result confirms that further mesh refinement will result in a negligible influence on solution accuracy

2.2. Model Validation

The numerical model was validated by simulating the flow of a fluid in a steady-state process through a smooth, circular tube under constant wall heat flux. Comparisons were performed against three references: an experimental one by Saood and Jalil[17], a numerical investigation carried out by Abdelmaksoud et al.[18], and classical analytical correlations provided by Dittus-Boelter equation for the Nusselt number and the Blasius equation for the friction factor[19]. Comparisons were made for Reynolds numbers in the range from 100 up to 15,000.

Figures 4 and 5 present the variation of Nusselt number and frication factor, respectively, with previous studies at different Reynolds numbers. Also, Table 4 summarize the error percentages of these two parameters. The present study shows strong agreement with the reference data. The deviation in the Nusselt number remained below 5.6% compared to the analytical solution, and under 4.2% compared to experimental data. The friction factor also followed the Blasius trend, with a maximum error of less than 5.3%. The validation confirms that the numerical model accurately captures the thermal and hydrodynamic behaviour of internal laminar flow, thus providing a reliable foundation for extending the study to more complex wavy tube geometries with time-varying wall heat flux.

Table 3. Summary of grid independent test of the developing section at Re=1500

Mesh	No. of elements	No. of nodes	Shear Stress	Error %	Nu	Error %	f	Error %
1	56520	63315	1.440	-	107.395	-	0.027	-
2	119320	126315	1.435	0.347	112.639	4.883	0.028	3.703
3	253600	265212	1.427	0.557	114.401	1.564	0.028	0.000
4	536320	552762	1.352	5.255	106.612	6.808	0.027	3.571
5	1192320	1222325	1.354	0.147	106.656	0.041	0.027	0.000
6	2347168	2395778	1.352	0.147	106.570	0.080	0.027	0.000
7	4350720	4427773	1.352	0.000	106.631	0.057	0.026	3.703

Table 4. Present study deviation compared with related studies

Ref.	Re	Nu	Error%	F	Error%
Present Developing Section	100-15000	5.3-106.7	0.30-0.16	0.64-0.02	0.79-0.05
Present Test section	100-5000	7.2-45.7	0.55-1.78	0.61-0.03	0.80-0.42
Saood and Jalil [15]	5000-15000	44.1-109.3	2.39-2.45	0.04-0.03	8.27-8.36
Abdelmaksoud et al. [16]	5000-15000	44-110.5	2.17-3.48	0.05-0.03	12.87-11.18
Dittus-Boelter eq. [17]	2500-15000	26.2-109.8	0.06-2.87	-	-
Blasius eq. [17]	2500-15000	-	-	0.05-0.03	13.47-5.24

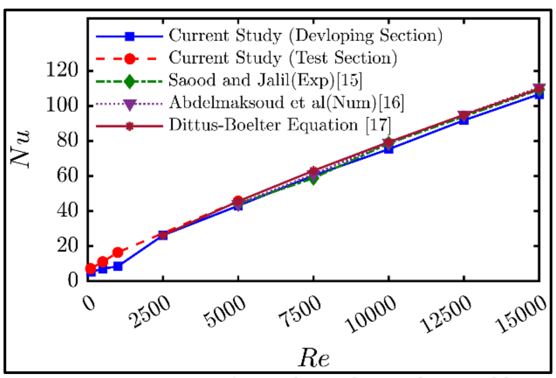

Figure 4. Variation of Nusselt number with Reynolds number compared to previous

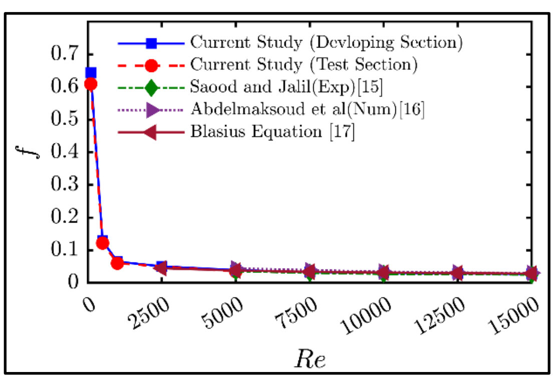

Figure 5. Variation of frication factor with Reynolds number compared to previous studies

3. Results and Discussion

3.1. Parametric study setup

A total of 27 simulations were performed by varying wave amplitude, wavelength, and tube length, as mentioned in Table 1 at a fixed Reynolds number of 5000. The objective was to assess the influence of each parameter on heat transfer and flow behaviour under a sinusoidal wall heat flux. Performance was evaluated using the surface-averaged Nusselt number and the thermal performance factor (TPF).

- *Effect of tube length:*

The length of the tube impacts the development of thermal and hydrodynamic boundary layers. Results in Figure 6 show that increasing the length generally reduces the Nusselt number, especially at low amplitude (h=0.1D), due to the development of a thermal layer and reduced downstream gradients. At higher amplitudes (h=0.2D, h=0.4D), Nu values were higher overall but exhibited similar decreasing trends beyond L = 20D. For example, at h3, Nusselt reached a maximum value of 88.83 for L= 20D and decreased further to 84.87 at L=40D. This shows that while increasing the tube length increases the surface area, the performance gets saturated as the flow gets thermally fully developed. Therefore, L=20D was optimal, providing a trade-off between the surface area and effective heat transfer.

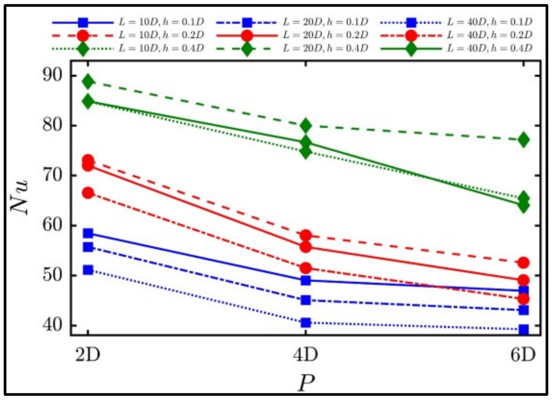

Figure 6. Effect of the tube geometrical scaled parameters on Nusselt number

- *Effect of wavelength:*

The thermal performance was evaluated at three wavelengths, as depicted in Figure 6. For all amplitudes and tube lengths considered in the study, the smallest wavelength (P = 2D) always yielded the largest Nusselt number due to the stronger secondary flows and wall mixing. For example, for L = 20D and h = 0.4D, the Nusselt number decreased from 88.83 with P = 2D to 80.00 and 77.18 with P = 4D and 6D, respectively.
Longer-wavelength diminishes flow disturbance by smoothening out the path and limiting expansion-contraction zones, weakening vortex strength and enhancing convective flow. This is more pronounced at high amplitudes where flow instabilities amplify mixing. Generally, shorter wavelengths enhance convective transport due to boundary layer disruption, which is exacerbated with larger amplitudes. The pressure drop that would result, however, should be considered in assessing the overall performance of the system.

- *Effect of wave amplitude:*

Wave amplitude has a significant impact on convective heat transfer because it disrupts the boundary layer and considerably enhances flow mixing. Three different amplitudes for different tube lengths and wavelengths were tested. An increase in amplitude was found to enhance the Nusselt number for all configurations tested, as depicted in Figure 6, since surface area increases along with more intense near-wall mixing. The enhancement was most significant for shorter wavelengths. For instance, in case L=10D, P=2D, Nu rose from 58.46 to 84.85 (≈ 45% increase); in L=20D, P2D, it increased from 55.74 to 88.83, representing the highest recorded improvement. This trend persisted across all oscillation periods, although relative gains were slightly lower at more extended periods, suggesting that higher amplitude is more effective under rapid oscillatory conditions with dominant unsteadiness. Among the 27 cases, the configuration with L=20D, P=2D, h=0.4 achieves a peak surface-averaged Nusselt number of 88.83, representing an enhancement of approximately 106% compared to the smooth tube, and a thermal performance factor (TPF) of 0.548 at Re = 5000.

To illustrate flow and thermal behaviour, velocity, temperature contours, and streamlines were generated for all configurations. Due to the large dataset, only two representative cases are shown in Table 5: the lowest and highest Nusselt number scenarios. Velocity contours, streamlines, and temperature fields were analysed in order to understand the physical mechanism responsible for their thermal performance. During case L40D-P6D-h0.1D, the flow remains mostly undeveloped and symmetric, with minimal interaction with the wall and a very weak gradient close to the boundary. Streamlines are basically parallel, with no evident recirculation, indicating poor mixing. Correspondingly, the temperature field depicts a thick, undisturbed thermal boundary layer, implying ineffective heat transfer and a nearly isothermal core. Heat transport is essentially performed by conduction; thus, the Nusselt number is the smallest of all the cases studied.

On the other hand, case L=20D-P=2D-h=0.4D expresses strong velocity gradients because of the wavy wall, where contractions and expansions could result in local acceleration and vortex formation. Streamlines show well-developed recirculation zones, enhancing the mixing of fluid between the wall and core. Thus, this acts like a disturbance to the thermal boundary layer by reducing thickness and increasing temperature gradient near the wall; this therefore enhances convective heat transfer, and the resulting Nusselt number is appreciably higher. The dynamic structure of the flow in L=20D-P=2D-h=0.4D facilitates continuous thermal boundary layer renewal and efficient heat redistribution throughout the fluid domain.

Table 5. Flow pattern for the highest and lowest average Nusselt numbers

	Velocity contour (m/s)	Velocity Streamline (m/s)	Temperature contour (K)
	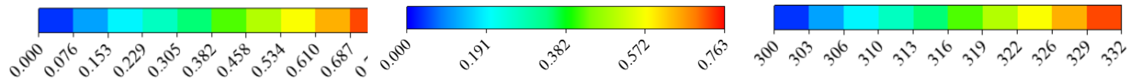		
L=40D P=6D h=0.1D	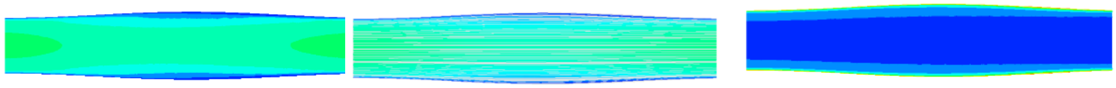		
L=20D P=2D h=0.4D	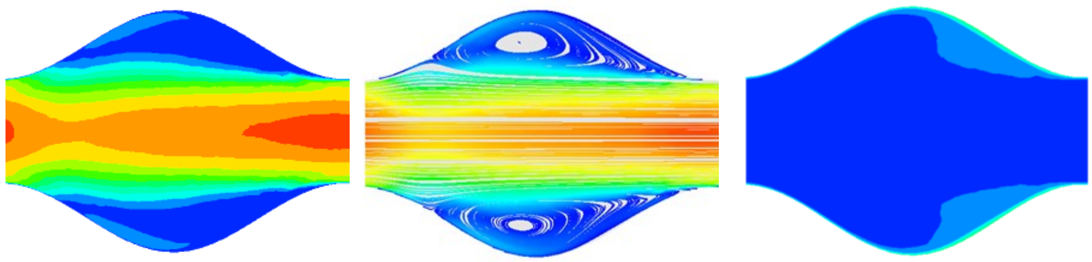		

3.2. Effect of Transient wall heat flux on the optimal configuration

After determining the best wavy tube geometry, represented by L=20D, P=2D, and h=0.4D, the investigations were extended to its performance under a transient wall heat flux. A sinusoidal heat flux[15]:

$$q(t) = q_m + A_q * sin\,(2\pi f_q\, t) \tag{5}$$

was applied, where q_m is the mean heat flux, A_q the amplitude, and f_q the forcing frequency. The goal was to investigate the interaction between unsteady thermal loading and the flow field within the optimized geometry, and to assess whether oscillatory heating could improve convective performance. Three amplitude levels (0.2, 0.5, and 0.8) representing increasing thermal excitation were tested. For each, four forcing frequencies were applied to capture frequency-dependent behaviour. This parametric analysis isolated the effect of thermal oscillations from geometric influences, offering insight into how time-dependent boundary conditions can be leveraged to enhance heat transfer in periodic-surface heat exchangers.

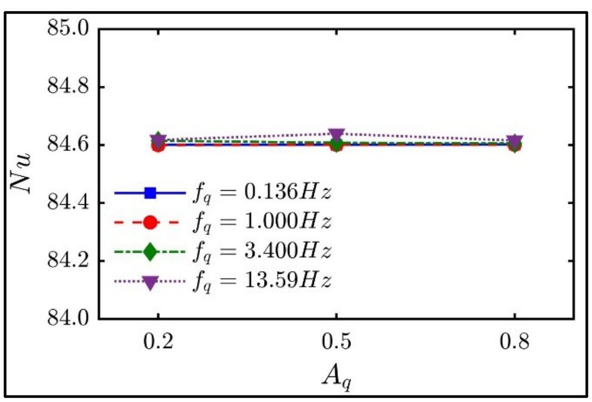

Figure 7. Effect of heat flux amplitude on the average Nusselt number for different frequencies

As shown in Figure 7, the results indicate that the average Nusselt number remains almost constant with increasing heat flux amplitude for all tested oscillation frequencies. This behaviour suggests that, within the examined amplitude range, the transient heat flux does not significantly alter the overall heat transfer mechanism in the wavy tube. Physically, this can be explained by the fact that the imposed oscillations in the wall heat flux affect only the instantaneous local wall temperature. At the same time, the time-averaged thermal boundary layer structure remains nearly unchanged. The dominant heat transfer process remains forced convection driven by bulk flow, and the small amplitude of the heat flux fluctuations does not induce sufficient unsteadiness to disturb the near-wall temperature gradient. This insensitivity can be attributed to three factors: (1) the fluid–solid system's thermal response is slower than the oscillation timescale, especially at higher frequencies; (2) the wavy geometry inherently promotes mixing and uniform heat transfer regardless of transient input; and (3) the symmetric oscillation around a constant mean result in no net change in thermal driving force over time. These findings suggest that the wavy tube maintains stable heat transfer behaviour even under unsteady thermal loading, with average performance dominated by the mean heat flux.

3.3. Evaluation of Thermal Performance Factor

The Thermal Performance Factor (TPF) assesses the trade-off between heat transfer enhancement and the associated hydraulic penalty. In this study, the TPF is calculated by comparing the average Nusselt number and friction factor of the wavy tube under sinusoidal heat flux with those of a smooth tube under steady conditions, as shown in Figures 8 and 9. The following correlation was used[19]:

$$TPF = \frac{Nu_{enhancement}}{Nu_{reference}} \Big/ \left(\frac{f_{enhancement}}{f_{reference}}\right)^{\frac{1}{3}} \quad (6)$$

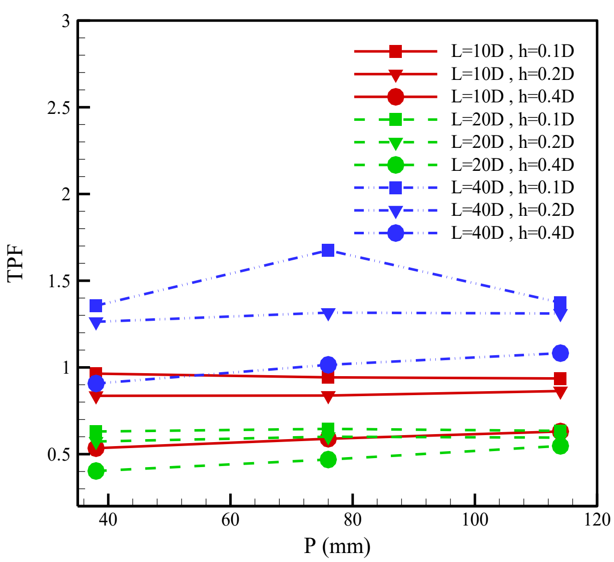

Figure 8. Variation of TPF with various tube geometrical scales

Figure 8 illustrates the variation of the thermal performance factor with wavelength for three wave amplitudes and tube lengths. Wave amplitude exerts the strongest influence on TPF. The values of TPF are maximum and close to unity for the smallest amplitude h = 0.1D with an optimum balance of frictional loss against heat transfer augmentation. In contrast, the TPF drops consistently with increasing wave amplitude to h = 0.2D and h = 0.4D, that is, when the extra pressure losses outweigh the corresponding thermal gains. This shows that excessive waviness reduces overall performance due to hydrodynamic costs, even while mixing is enhanced.

The wavelength also affects the wave, especially when the wave amplitude is low. Tube length has a secondary impact; for a given design, increasing L does not change the qualitative dependence on P and h, but it somewhat reduces TPF due to accumulated frictional losses. Overall, the figures show that waviness $h = 0.1D$ and moderate wavelength $P = 4D$, especially at $L = 40D$, yield the optimum thermal–hydraulic balance. In contrast, the configuration with the largest Nusselt number ($L = 20D$, $P = 2D$, $h = 0.4D$) has a very low TPF due to the dominance of its frictional loss

4. Conclusion

The thermal and hydrodynamic performance of a wavy tube heat exchanger exposed to both constant and time-varying heat fluxes was assessed in this work using a comparative numerical analysis. The novelty of the present study lies in the application of a time-varying sinusoidal heat flux to a wavy tube heat exchanger and in the assessment of its interaction with the tube geometry under transient conditions, extending previous studies that mainly considered steady thermal boundary conditions. The tube lengths (three values), wave amplitude (three values), and wavelength (three values) were varied in a parametric investigation of wavy tubes. The results showed that the best-performing wavy geometry achieved a 106.5% increase in the average Nusselt number compared to the smooth tube. In contrast, the worst-performing case showed a 9.3% decrease, highlighting that improper geometric ratios can have a negative impact on thermal performance. A transient periodic heat flux was used in heating the wavy walls to examine its effect on the thermal performance. The findings showed that there is no considerable effect of the heat flux fluctuating on the rate of heat enhancement. This comparison between constant and time-varying heat flux conditions indicates that the overall enhancement of heat transfer is dominated by its mean value rather than instantaneous oscillations. Also, the TPF has improved in some of the studied configurations. The optimum case was for L, P, and h equal to 40D, 4D, and 0.1D, respectively. Therefore, configuration analysis improved the overall hydrothermal performance. All these results clearly show the highlight of the contribution in the present work, i.e., the assessment of wavy tube geometry combined with time-varying sinusoidal heat flux, with quantitative comparisons of both thermal and hydrodynamic performance. Based on the results obtained in the present study, further work might also be performed by considering different time-dependent heat flux profiles (e.g., exponential or non-sinusoidal functions), besides the sinusoidal type used here. Moreover, extending the analysis to other working fluids can provide wider perspectives on the applicability of the proposed configuration. Furthermore, future studies can focus on a triple product boundary condition problem in which wavy tubes, time-dependent wall heat fluxes, and oscillatory flows can be considered.

Nomenclature

Aq	Amplitude of heat flux
Cp	Specific heat (J/kg. K)
f	Friction factor
f_q	Frequency (Hz)
h	Wave amplitude
K	Thermal conductivity (W/m. K)
L	Tube length
Nu	Nusselt number
P	Pitch (wavelength)
P/D	Pitch-to-diameter ratio
Pr	Prandtl number
PR	Pressure ratio
q_m	Mean heat flux
Re	Reynolds number
TPF	Thermal performance factor
τ	Stress tensor
μ	Dynamic viscosity (kg/m.s)
ρ	Density (kg/m^3)

Funding
None

Conflicts of Interest
None

Appendix
None.

References

[1] A. G. Ramgadia and A. K. Saha, "Fully developed flow and heat transfer characteristics in a wavy passage: Effect of amplitude of waviness and Reynolds number," *Int. J. Heat Mass Transf.*, vol. 55, no. 9–10, pp. 2494–2509, 2012, doi: 10.1016/j.ijheatmasstransfer.2012.01.010.

[2] H. Bai, Z. Lin, M. M. Alam, and F. Zhao, "Near wake flow and forced convection heat transfer of sinusoidal wavy cylinder based on flow decomposition," *Int. J. Heat Mass Transf.*, vol. 202, 2023, doi: 10.1016/j.ijheatmasstransfer.2022.123753.

[3] Z. X. Wen, J. L. Wu, S. S. Wang, J. Q. Cheng, and Q. Li, "Numerical study and machine learning on local flow and heat transfer characteristics of supercritical carbon dioxide mixtures in a sinusoidal wavy channel PCHE," *Int. J. Heat Mass Transf.*, vol. 223, no. February, 2024, doi: 10.1016/j.ijheatmasstransfer.2024.125278.

[4] A. Ahmadpour and S. M. A. Noori Rahim Abadi, "Thermal-hydraulic performance evaluation of gas-liquid multiphase flows in a vertical sinusoidal wavy channel in the presence/absence of phase change," *Int. J. Heat Mass Transf.*, vol. 138, pp. 677–689, 2019, doi: 10.1016/j.ijheatmasstransfer.2019.04.084.

[5] L. Zhang *et al.*, "Analysis of nanofluid flow and heat transfer characteristics in a wavy-walled tube heat exchanger," *Int. J. Heat Fluid Flow*, vol. 108, no. June, 2024, doi: 10.1016/j.ijheatfluidflow.2024.109488.

[6] A. R. Al-Obaidi, "Investigation of fluid field analysis, characteristics of pressure drop and improvement of heat transfer in three-dimensional circular corrugated pipes," *J. Energy Storage*, vol. 26, no. October, 2019, doi: 10.1016/j.est.2019.101012.

[7] L. Zhang *et al.*, "Heat transfer and flow characteristics of fluids in wavy-walled tubes under the combined effect of vibrations and pulsations," *Appl. Therm. Eng.*, vol. 268, no. December 2024, 2025, doi: 10.1016/j.applthermaleng.2025.125853.

[8] J. I. Córcoles, J. D. Moya-Rico, A. E. Molina, and J. A. Almendros-Ibáñez, "Numerical and experimental study of the heat transfer process in a double pipe heat exchanger with inner corrugated tubes," *Int. J. Therm. Sci.*, vol. 158, no. May, 2020, doi: 10.1016/j.ijthermalsci.2020.106526.

[9] A. R. Al-Obaidi and J. Alhamid, "Investigation of flow pattern, thermohydraulic performance and heat transfer improvement in 3D corrugated circular pipe under varying structure configuration parameters with development different correlations," *Int. Commun. Heat Mass Transf.*, vol. 126, no. June, 2021. doi: 10.1016/j.icheatmasstransfer.2021.105394.

[10] H. S. Yoon, S. H. Nam, and M. Il Kim, "Laminar forced convection heat transfer around wavy elliptic cylinders with different aspect ratios," *Int. J. Heat Mass Transf.*, vol. 194, 2022, doi: 10.1016/j.ijheatmasstransfer.2022.123038.

[11] S. K. Mehta and S. Pati, "Numerical study of thermo-hydraulic characteristics for forced convective flow through wavy channel at different Prandtl numbers," *J. Therm. Anal. Calorim.*, vol. 141, no. 6, pp. 2429–2451, 2020, doi: 10.1007/s10973-020-09412-5.

[12] G. Russ and H. Beer, "Heat transfer and flow field in a pipe with sinusoidal wavy surface - I. Numerical investigation," *Int. J. Heat Mass Transf.*, vol. 40, no. 5, pp. 1061–1070, 1997, doi: 10.1016/0017-9310(96)00158-5.

[13] M. Sun and M. Zeng, "Investigation on turbulent flow and heat transfer characteristics and technical economy of corrugated tube," *Appl. Therm. Eng.*, vol. 129, pp. 1–11, 2018, doi: 10.1016/j.applthermaleng.2017.09.136.

[14] M. M. Ahmed and A. Trouvé, "Simulations of the unsteady response of biomass burning particles exposed to oscillatory heat flux conditions," *Fire Saf. J.*, vol. 120, no. January 2020, 2021, doi: 10.1016/j.firesaf.2020.103059.

[15] A. R. A. Khaled, "Conduction heat and entropy transfer in a semi-infinite medium and wall with a combined periodic heat flux and convective boundary condition," *Int. J. Therm. Sci.*, vol. 47, no. 1, pp. 76–83, 2008, doi: 10.1016/j.ijthermalsci.2007.01.011.

[16] S. M. Jalil, "Mathematical and numerical predictions for optimum perfect mixing by bulk convective oscillatory exchange," *Int. J. Heat Mass Transf.*, vol. 167, p. 120792, 2021, doi: 10.1016/j.ijheatmasstransfer.2020.120792.

[17] M. M. Saood and S. M. Jalil, "Effect of Vortex Generators in Accelerating the Thermal Diffusion Inside the Stokes Boundary Layer," *AIP Conf. Proc.*, vol. 3009, no. 1, 2024, doi: 10.1063/5.0190514.

[18] W. A. Abdelmaksoud, A. E. Mahfouz, and E. E. Khalil, "Thermal Performance Enhancement for Heat Exchanger Tube Fitted with Vortex Generator Inserts," *Heat Transf. Eng.*, vol. 42, no. 21, pp. 1861–1875, 2021, doi: 10.1080/01457632.2020.1826743.

[19] M. Mobedi and G. Gediz Ilis, *Fundamentals of Heat Transfer*. 2023. doi: 10.1007/978-981-99-0957-5.